2008

# Simulation and Validation of a Two-Stage Flash Tank Cycle Using R410A as a Refrigerant

Jonathan Winkler
*University of Maryland*

Xudong Wang
*Air-Conditioning*

Vikrant Aute
*University of Maryland*

Reinhard Radermacher
*University of Maryland*

# Simulation and Validation of a Two-Stage Flash Tank Cycle using R410A as a Refrigerant

Jon WINKLER[1]*, Xudong WANG[2], Vikrant AUTE[3], Reinhard RADERMACHER[4]

[1,3,4]Center for Environmental Energy Engineering
Department of Mechanical Engineering, University of Maryland
College Park, MD 20742 USA
[1,3]Tel: 301-405-8726, [4]Tel: 301-405-5286, Fax: 301-405-2025
Email: [1]jwinkler@umd.edu, [3]vikrant@umd.edu, [4]raderm@umd.edu

[2]Air-Conditioning, Heating, and Refrigeration Institute
4100 N. Fairfax Drive, Ste 200
Arlington, VA 22203-1678
Tel: 703-600-0305, Fax: 703-522-2349
Email: xwang@ahrinet.org

*Corresponding Author.

## ABSTRACT

Investigating alternative system configurations is a means to improving vapor compression system COP by increasing system capacity and reducing compressor power consumption. The characterization and optimization of alternative system configurations can be conducted through the use of simulation. This paper presents a vapor compression system simulation tool capable of modeling a two-stage flash tank cycle. The key component model in the simulation of a two-stage flash tank cycle is the compressor. The component-based nature of the simulation tool allows for the use of any type of two-stage compressor model, including a vapor-injection compressor. The simulation assumptions and approach are presented in this paper. The experimental validation for both the baseline cycle and flash tank cycle are presented for an R410A system operating in both heating and cooling modes. A total of 52 test points were included in the validation for the two operating modes. The calculated capacity for 48 of the 52 test points was predicted to within 5% of experimental values.

## 1. INTRODUCTION

Vapor compression heat pumps provide space cooling during summer months and heating during winter months. While nearly all modern-day homes in the U.S. utilize a heat pump to provide cooling during the summer, the use of a heat pump to provide heating during the winter is limited to homes located in climates with relatively moderate winters. This is due to the fact that vapor compression system capacity and coefficient of performance (COP) significantly degrade at extreme ambient conditions (i.e. when the ambient temperature peaks during the summer months and is coldest during the winter months). During extreme winter conditions the diminished capacity is often supplemented through the use of electrical resistance heating, which cannot compete with the COP of a vapor compression system. Alternative system configurations, such as a two-stage vapor injection flash tank cycle, could prove useful at mitigating capacity degradation at extreme ambient conditions.

A typical vapor compression heat pump system, as shown in Figure 1, consists of five components; namely a compressor, outdoor heat exchanger, expansion valve, indoor heat exchanger, and four-way switching valve. When operating in cooling mode, compressed vapor refrigerant passes through the four-way valve on its way to the outdoor heat exchanger. In the outdoor heat exchanger the refrigerant rejects heat to the outdoor environment and is condensed prior to being throttled in the expansion valve. While flowing through the indoor heat exchanger, the refrigerant absorbs heat from the indoor environment and is evaporated to a superheated state prior to flowing back through the four-way valve immediately before the compressor suction port. When in the heating mode the four-way valve switches position reversing the flow of refrigerant through the system. The compressed refrigerant rejects heat while flowing through the indoor heat exchanger and absorbs heat from the outdoor environment.

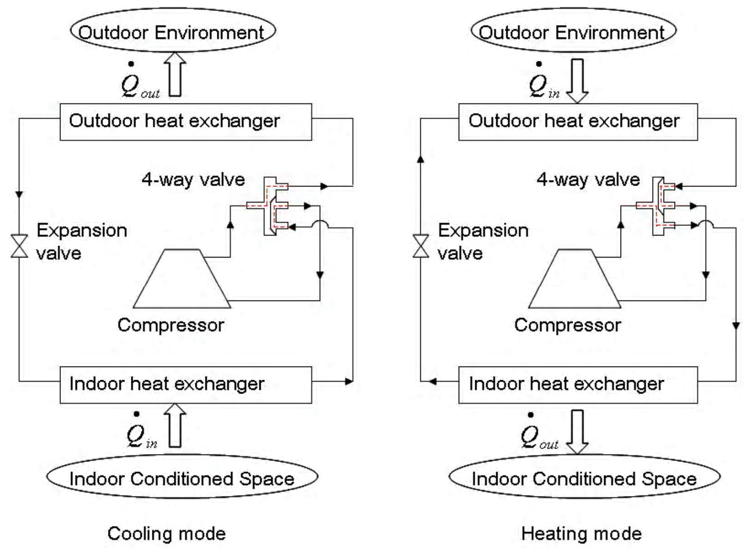


Figure 1: Diagram of a typical vapor compression heat pump

A two-stage flash tank cycle (FTC), as shown in Figure 2a, contains two additional components compared to the standard vapor injection cycle, namely an additional expansion valve and a flash tank separator. The corresponding cycle plotted on a P-h diagram is shown in Figure 2b. In a two-stage flash tank cycle the condensed liquid leaving the condenser is first throttled through the first stage expansion device and the two-phase refrigerant (state point 4) enters in the flash tank separator. In the flash tank the liquid and vapor components of the two-phase mixture are separated. The saturated vapor refrigerant is injected at an intermediate compressor suction port and the saturated liquid refrigerant is throttled through the second stage expansion device prior to entering the evaporator.

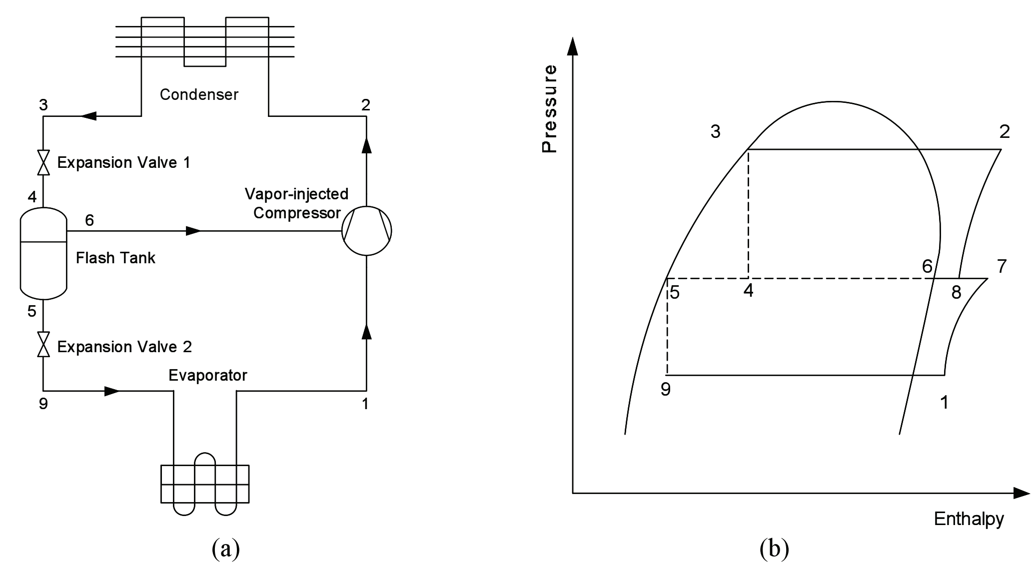


Figure 2: Diagram of a two-stage flash tank cycle

The two-stage flash tank cycle has been used to enhance system performance for refrigeration systems; however, the benefit to residential heat pump systems remains a current research topic. Simulation can aid in characterizing the system performance of the two-stage flash tank cycle and a validated model must be developed prior to using simulation as an optimization tool. This paper presents the modeling procedure and validation results of a R410A 11 kW residential two-stage vapor injection flash tank cycle. The modeling procedure and results from the baseline system simulation are also included.

## 2. MODELING PROCEDURE

Simulation of the baseline system and the two-stage flash tank cycle were conducted using similar approaches; however due to the difference in the system configuration for the two systems, a separate solution technique was developed for the two-stage flash tank cycle. The simulation procedure implemented a component-based approach, and thus a short overview of the component-based nature of the simulation tool will be discussed.

### 2.1. Component-Based Simulation

The component-based approach used to simulate a vapor compression system has been described by Winkler *et al.* (2006). In this approach, the component models contain the appropriate engineering equations for that particular model and are treated like "black-box" objects by the system solver. The system solver communicates with the component models through the use of a component-based framework. Thus once the input parameters have been set to each component model, the system solver must only set the component boundary conditions prior to executing the component model and then after execution use the output parameters to complete the system simulation. For this reason, the system solution procedure can be discussed without describing the details and assumptions of each component model. The component model input parameters will be presented in the validation section of this paper.

### 2.2. Baseline Cycle

The baseline system is a standard four component vapor compression system as shown in Figure 3a. For this study, the pressure drop and heat transfer effects of the four-way switching valve were neglected, and the cooling and heating modes were modeled by switching the corresponding input parameters for the condenser and evaporator. The procedure used to simulate the baseline system is described in detail by Winkler *et al.* (2007) and thus the reader is referred to this paper for a more complete description of the solution algorithm.

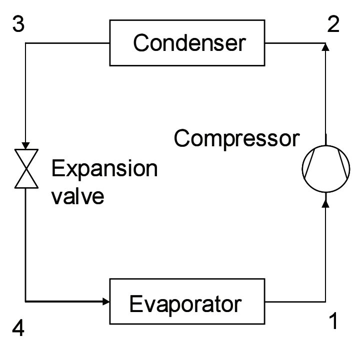


$$\vec{x} = \begin{bmatrix} P_1 \\ P_2 \\ P_3 \\ P_4 \\ h_1 \end{bmatrix} \qquad \vec{r} = \begin{bmatrix} \dot{m}_{ExpValve} - \dot{m}_{Comp} \\ \dot{m}_{ExpValve} h_{Evap,out} - \dot{m}_{Comp} h_1 \\ P_{Evap,1,out} - P_1 \\ P_{Cond,out} - P_3 \\ h_{SC} - h_{Cond,out} \end{bmatrix}$$

(a) (b) (c)

Figure 3: (a) Diagram of basic vapor compression system, (b) vector of unknown variables, and (c) corresponding set of residual equations for the baseline system

For the baseline system, the state point pressures and suction enthalpy are chosen as the unknown parameters that are iteratively solved for by the system solver. The remaining state point enthalpies and the system mass flow rate are calculated as the solution procedure iterates. The unknown variables can be placed in a vector as shown in Figure 2b, which is filled with an initial guess solution at the start of the solution procedure.

The solution procedure starts with running the compressor using the suction enthalpy ($h_1$) and the suction and discharge pressures ($P_1$ and $P_2$). The calculated compressor mass flow rate and discharge enthalpy are propagated to the condenser prior to the model being executed. The condenser calculates the enthalpy at state point 3 and an outlet pressure using pressure drop correlations. Using the pressure at state point 3 ($P_3$) and the outlet enthalpy of the condenser, the expansion valve calculates a mass flow rate. The expansion valve mass flow rate and outlet enthalpy along with the pressure at state point 4 ($P_4$) are then used to run the evaporator. The evaporator calculates an outlet enthalpy and pressure. The calculated output from the component models are used in formulating a vector of residual values, shown in Figure 2c, which represent the set of equations being solved to determine the set of unknown values.

A final residual must be used to close the set of unknowns. For this case the system subcooling has been chosen to close the set of equations and thus a value for the subcooling must be input to the solution algorithm. The enthalpy used in calculating this residual ($h_{SC}$) is determined by Equation 1, where $T_{SC}$ is the degree of subcooling input to the system solver.

$$h_{SC} = f\left(P = P_3, T = T_{sat@P3} - T_{SC}\right) \tag{1}$$

The set of unknown values are simultaneously adjusted by a nonlinear equation solver until the residuals satisfy a specified tolerance.

$$\left\|\vec{r}\left(\vec{x}\right)\right\|_2 \le \varepsilon_f \tag{2}$$

## 2.3. Vapor Injected Compressor Model

The baseline system used a single stage scroll compressor and therefore was modeled using manufacturer data along with the compressor polynomial equation provided by ARI Standard 540-1999. However due to the experimental phase of the two-stage vapor injection compressor used in the flash tank cycle, manufacturer data (and a corresponding compressor standardized equation) were not available. Thus, the vapor injection scroll compressor was modeled as a two stage compressor model, as shown in Figure 4, with a volume ratio of 0.75. The displacement volume of the low stage was equivalent to the displacement volume of the baseline compressor and the volume ratio was defined as the ratio of the high stage displacement volume to the low stage displacement volume. The volumetric and isentropic efficiencies of both the low and high stages were calculated using experimental results and were used to generate compressor maps for the low and high stages according to ARI Standard 540-1999. The isentropic and volumetric efficiencies for the low stage were calculated using the evaporating and condensing temperature, as shown in Equation 3, whereas the isentropic and volumetric efficiencies for the high stages were calculated using the injection and condensing temperatures, as shown in Equation 4.

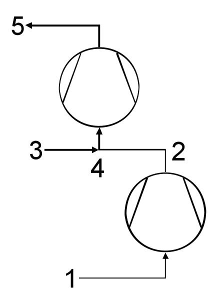

Figure 4: Diagram of a two stage vapor injection compressor model

Table 1: Two stage compressor model inputs and outputs

| Inputs | Outputs |
|---|---|
| $P_1$ | $\dot{m}_{low}$ |
| $P_3$ | $\dot{m}_{inj}$ |
| $P_5$ | $\dot{m}_{high}$ |
| $h_1$ | $h_5$ |
| $h_3$ | $\dot{P}_{total}$ |

$$\begin{aligned}\eta)_{low} &= c_1 + c_2 T_{sat,1} + c_3 T_{sat,5} + c_4 T_{sat,1}^2 + c_5 T_{sat,5}^2 + c_6 T_{sat,1} T_{sat,5} + \\ & c_7 T_{sat,1}^3 + c_8 T_{sat,5}^3 + c_9 T_{sat,1} T_{sat,5}^2 + c_{10} T_{sat,1}^2 T_{sat,5}\end{aligned} \tag{3}$$

$$\begin{aligned}\eta)_{high} &= c_1 + c_2 T_{sat,3} + c_3 T_{sat,5} + c_4 T_{sat,3}^2 + c_5 T_{sat,5}^2 + c_6 T_{sat,3} T_{sat,5} + \\ & c_7 T_{sat,3}^3 + c_8 T_{sat,5}^3 + c_9 T_{sat,3} T_{sat,5}^2 + c_{10} T_{sat,3}^2 T_{sat,5}\end{aligned} \tag{4}$$

Using the displacement volume, compressor speed, isentropic and volumetric efficiency for each stage along with the input conditions listed in Table 1, the corresponding compressor outputs were calculated. The compressor model requires an iterative solution procedure to resolve the injection and discharge mass flow rates along with the suction enthalpy of the high stage, $h_4$. The suction enthalpy of the high stage is calculated according to Equation 5 and the compressor model assumes that the refrigerant pressures at state points 2, 3, and 4 within the compressor are equal.

$$h_4 = \frac{\dot{m}_{low} h_2 + \dot{m}_{inj} h_3}{\dot{m}_{high}} \tag{5}$$

### 2.4. Vapor Injected Flash Tank Cycle

The simulation procedure used to model the vapor injection flash tank cycle, as shown in Figure 5a, differs from the basic vapor compression system due to the constraint placed on the system by the assumption used to model the flash tank component. The flash tank component was modeled assuming saturated vapor ($x_5 = 1$) enters the intermediate suction port of the compressor and saturated liquid ($x_4 = 0$) enters the low stage expansion valve. During the experimental investigation of the flash tank cycle, it was determined that the flash tank performance was very sensitive to the high stage expansion valve setting. If the high stage expansion device was not set within a very narrow range, the flash tank would either completely fill with liquid refrigerant or completely drain of liquid refrigerant. Since the flash tank performance was highly dependent on the high stage expansion valve diameter, it was determined that the high stage expansion valve diameter should be output from the system simulation. Therefore, the high stage expansion valve and flash tank were lumped together in a single component model. The high stage expansion valve diameter was calculated using the compressor discharge mass flow rate and assuming saturated vapor and saturated liquid were exiting the flash tank at a pressure of $P_5$. The pressure drop through the flash tank was neglected, and thus the pressure at the inlet to low stage expansion valve was set equal to $P_5$.

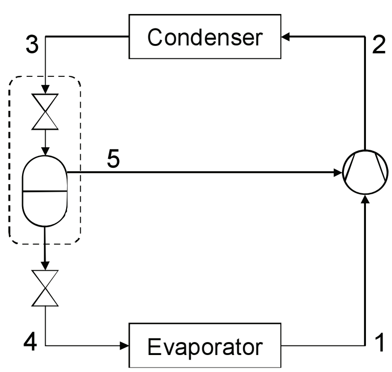


(a)

$$\vec{x} = \begin{bmatrix} P_1 \\ P_2 \\ P_3 \\ P_4 \\ P_5 \\ h_1 \end{bmatrix}$$

(b)

$$\vec{r} = \begin{bmatrix} h_1 - h_{evap,out} \\ \dot{m}_{exp,low} - \dot{m}_{suction} \\ \dot{m}_{flash,vap} - \dot{m}_{injection} \\ P_3 - P_{cond,out} \\ P_1 - P_{evap,out} \\ h_{SC} - h_{cond,out} \end{bmatrix}$$

(c)

Figure 5: (a) Diagram of flash tank cycle, (b) vector of unknown variables, and (c) corresponding set of residual equations for the flash tank cycle

Similar to the baseline system, the state point pressures and suction enthalpy are chosen as the unknown parameters that are iteratively solved for by the system solver. The injection enthalpy is required to execute the compressor model; however the injection enthalpy is easily calculated using the flash tank modeling assumption that saturated vapor is being injected into the compressor. The remaining state point enthalpies and the system mass flow rate are calculated as the solution procedure iterates.

Similar to the simulation of the baseline system, solution to the flash tank cycle commences with the execution of the compressor model using the suction enthalpy and pressure ($h_1$ and $P_1$), injection enthalpy and pressure ($h_5$ and $P_5$), and the discharge pressure ($P_2$). The calculated compressor discharge mass flow rate and enthalpy are propagated to the condenser. The condenser calculates the enthalpy at state point 3 and an outlet pressure using pressure drop correlations. The high stage expansion valve/flash tank component is then run using the pressure at state point 3 ($P_3$), the condenser outlet enthalpy, compressor discharge mass flow rate, and pressure at state point 5 ($P_5$). The low stage expansion valve calculates a low side mass flow rate using the pressure at state point 5 ($P_5$) and corresponding saturated liquid enthalpy along with the pressure at state point 4 ($P_4$). The expansion valve mass flow rate and outlet enthalpy along with the pressure state point 4 ($P_4$) are then used to run the evaporator. The evaporator calculates an outlet enthalpy and pressure. Similar to the simulation of the baseline system a set of residual equations are calculated, as shown in Figure 5c.

## 3. SIMULATION VALIDATION RESULTS

### 3.1. Simulation Input Parameters

An 11 kW R410A residential system with a scroll compressor was tested at two cooling mode operating points and three heating mode operating points according to ASHRAE Standard 37-2005. The system was also tested at an extended condition, which were an extreme high temperature for the cooling mode and an extreme low temperature for the heating mode. The operating test conditions are summarized in the Table 2. The baseline system was tested at three additional operating points and the flash tank cycle was tested at various injection pressures for each operating point. In total, the baseline system was tested at 10 operating points (4 cooling and 6 heating) and the flash tank cycle was tested at 42 operating points (24 cooling and 18 heating).

Table 2: ASHRAE test conditions and extended condition

| **Cooling** | | | | | **Heating** | | | | |
|---|---|---|---|---|---|---|---|---|---|
| **Test** | **Indoor** | | **Outdoor** | | **Test** | **Indoor** | | **Outdoor** | |
| | DB(°C) | WB(°C) | DB(°C) | WB(°C) | | DB(°C) | WB(°C) | DB(°C) | WB(°C) |
| A | 26.7 | 19.4 | 35.0 | N/A | High 1 | 21.1 | ≤15.6 | 16.7 | 14.7 |
| B | | | 27.8 | | High 2 | | | 8.3 | 6.1 |
| Extended | | | 46.1 | | Low | | | -8.3 | -9.4 |
| | | | | | Extended | | | -17.8 | N/A |

The indoor and outdoor heat exchangers were simulated using CoilDesigner, a heat exchanger simulation tool originally presented by Jiang (2003), and the details concerning the heat exchanger parameters can be found in Wang (2008). As mentioned in Section 2.3, the baseline compressor was modeled using manufacturer data and the vapor injected compressor was modeled using experimental results. Each operating point was simulated using the experimental subcooling and superheat as input.

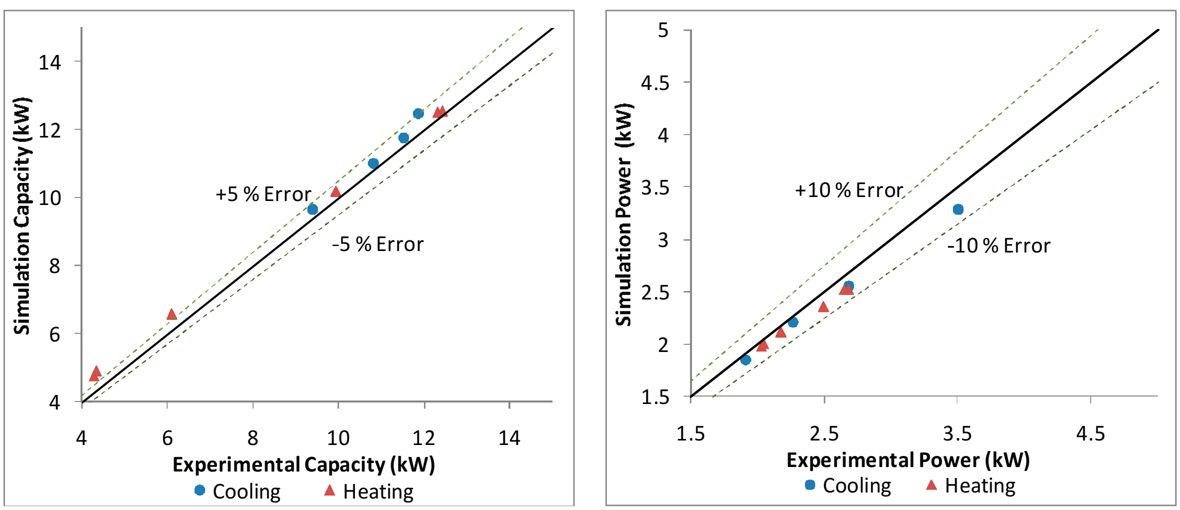


(a) (b)

Figure 6: Baseline cycle validation results for (a) system capacity and (b) compressor power consumption

### 3.2. Baseline Cycle Simulation Results

The system capacity and power consumption validation results for the baseline system are shown in Figure 6. The average relative error in the system capacity was 4.8% with a maximum error of 12.4%. The system capacity of 8 of the 10 operating points was predicted to within ±5%; however in all cases the capacity was over predicted by the simulation. The compressor power was simulated with an average error 4.2% with a maximum relative error of

6.5%. The compressor power consumption was under predicted for all the operating points and the error in the power consumption was less than 5% for 7 of the 10 cases. The operating points with the largest error were the high ambient cooling case and the lowest ambient heating cases. The manufacturer coefficients for this model were generated using test data at an ambient temperature of 35°C. Since the heat transfer between the compressor shell and the ambient was neglected, there is a high amount of error in the compressor simulation when the ambient temperature is significantly different from 35°C. As shown in Figure 7a, the simulation accurately predicts the system mass flow rate with an average error of 3.4% and a maximum relative error of 7.2%.

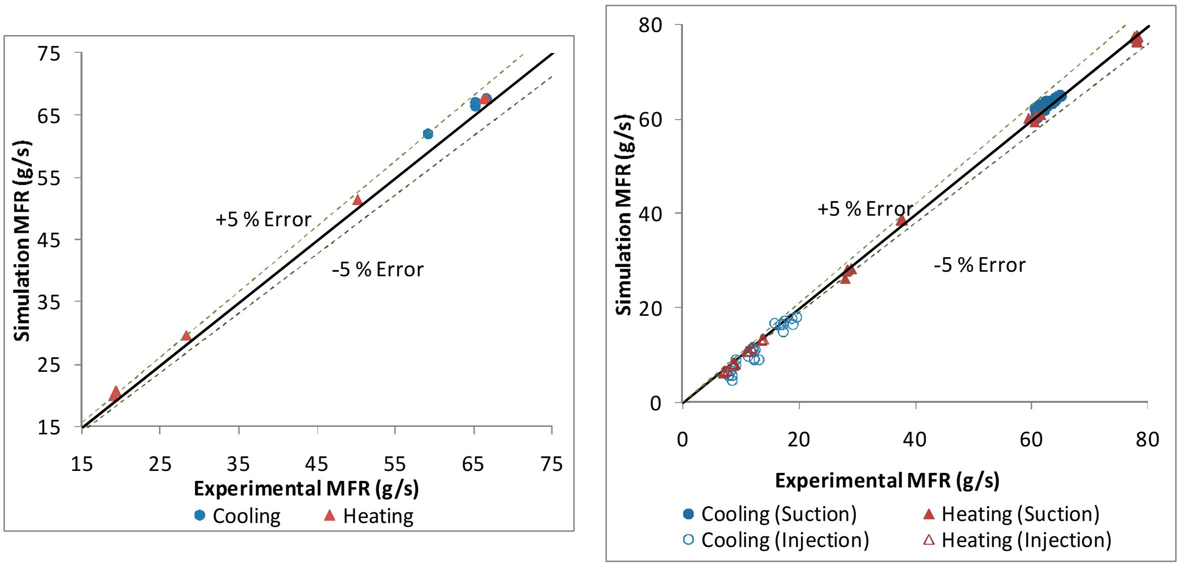


(a) (b)

Figure 7: Mass flow rate results for the (a) baseline system and (b) flash tank cycle

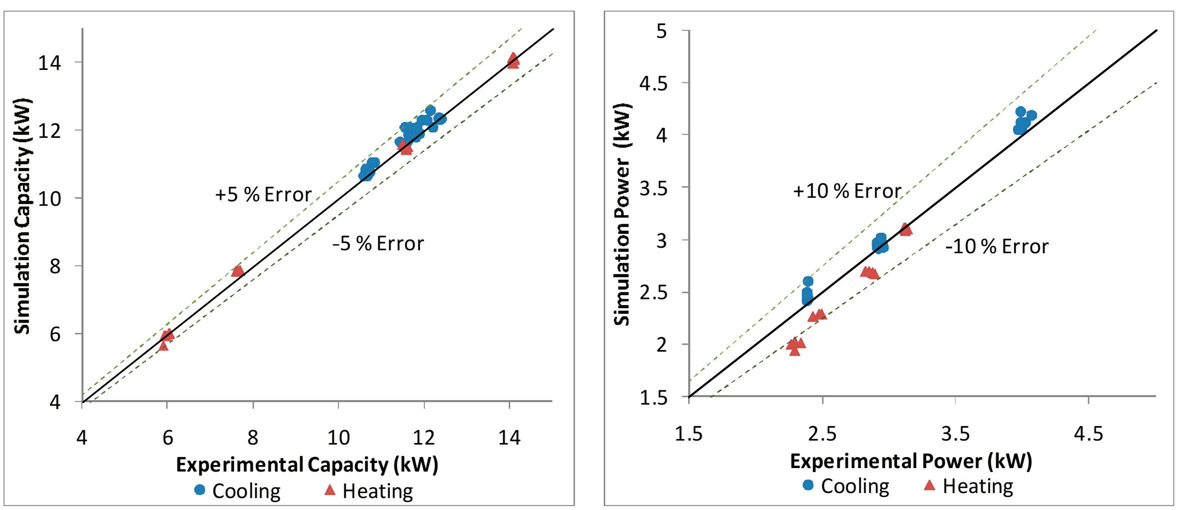


(a) (b)

Figure 8: Flash tank cycle validation results for (a) system capacity and (b) compressor power consumption

### 3.3. Flash Tank Cycle Simulation Results

The system capacity and power consumption validation results for the flash tank cycle are shown in Figure 8. The average relative error in the system capacity was 1.3% with a maximum error of 4.5% and 31 of the 42 points falling within ±2%. The compressor power consumption was predicted with an average relative error of 4.0% with a maximum error of 15.3% and 29 of the 42 points falling within ±5%. Similar to the baseline system, the points with the most significant error were those operating points with the highest and lowest ambient temperatures. Figure 7b shows the suction and injection mass flow rates for the flash tank cycle. The suction mass flow rate was predicted with an average relative error of 1.2% and a maximum relative error of 6.1% with 38 of the 42 points falling within ±3% of the experimental values. The injection mass flow rate was not as accurately predicted and had an average relative error of 10.3% and a maximum relative error of 45.6%. The maximum relative error corresponds to an absolute error of 3.9g/s, which does significantly affect the discharge mass flow rate. The high error of the simulated injection mass flow rate could have been a result of the flash tank modeling assumption of ideal phase separation. Even though site glasses were used in the experiment to ensure saturated vapor was being injected into the compressor, it is possible that the injected refrigerant was indeed a high quality two phase mixture which results in a higher injection mass flow rate due to the increase in the injection refrigerant density.

# 4. CONCLUSIONS

In this paper, a system simulation algorithm for a flash tank cycle has been discussed. The system level variables and corresponding equation set have been formulated. The modeling procedure for the two stage vapor injection scroll compressor has been introduced. A validation using a total of 52 experimental operating points for the baseline system and the flash tank cycle have been presented. The flash tank cycle capacity was predicted with an average relative error of 1.3% and 31 of the 42 points were predicted within ±2% of the experimental capacity.

# NOMENCLATURE

| | | | | | |
|---|---|---|---|---|---|
| $c_i$ | Coefficient | (-) | WB | Wet Bulb Temperature | (°C) |
| DB | Dry Bulb Temperature | (°C) | $\vec{x}$ | Vector of Unknown Values | (-) |
| $h$ | Enthalpy | (J/kg) | $\varepsilon_f$ | Tolerance | (-) |
| $\dot{m}$ | Mass Flow Rate | (kg/s) | $\eta$ | Isentropic/Volumetric Efficiency | (-) |
| $P$ | Pressure | (Pa) | | **Subscripts** | |
| $\dot{P}$ | Power Consumption | (W) | g | Saturated Vapor | |
| $\vec{r}$ | Vector of Residual Values | (-) | sat | Saturation | |
| $T$ | Temperature | (°C) | SC | Subcooling | |

# REFERENCES

ANSI/ARI Standard 540-1999, 1999, "Positive Displacement Refrigerant Compressors and Compressor Units", Air-Conditioning and Refrigeration Institute, Arlington, VA

ASHRAE Standard, 2005, Methods of testing for rating electrically driven unitary air-conditioning and heat pump equipment, ANSI/ASHRAE Standard 37-2005

Jiang, H., Aute, V., Radermacher, R., 2006, "CoilDesigner: A General Purpose Simulation and Design Tool for Air-to-Refrigerant Heat Exchangers", *International Journal of Refrigeration*, Vol. 29, p. 601-610

Wang, X., Performance Investigation of Two-Stage Heat Pump System with Vapor-Injection Scroll Compressor", Ph.D. Thesis, Dept. of Mechanical Engineering, University of Maryland, College Park, MD, 2008.

Winkler, J., Aute, V., and Radermacher, R., 2006, "Component-Based Vapor Compression Simulation Tool with Integrated Multi-Objective Optimization Routines", *International Refrigeration and Air Conditioning Conference at Purdue*, Purdue University, July 2006.

Winkler, J., Aute, V., and Radermacher, R., 2007, "Comprehensive Investigation of Numerical Methods in Simulating a Steady State Vapor Compression System", *International Journal of Refrigeration*, doi:10.1016/j.ijrefrig.2007.08.008.